



Lithium polyacrylate as a binder for tin–cobalt–carbon negative electrodes in lithium-ion batteries

Jing Li^a, Dinh-Ba Le^b, P.P. Ferguson^c, J.R. Dahn^{a,c,*}

^a Dept. of Chemistry, Dalhousie University, Halifax, N.S. B3H 3J5, Canada

^b 3M Electronic Markets Materials Division, 3M Center, St. Paul, MN 55144-1000, USA

^c Dept. of Physics and Atmospheric Science, Dalhousie University, Halifax, N.S. B3H 3J5, Canada

ARTICLE INFO

Article history:

Received 23 October 2009

Received in revised form 5 January 2010

Accepted 6 January 2010

Available online 15 January 2010

Keywords:

Binder

Tin–cobalt–carbon

Negative electrode

Lithium polyacrylate

Li-ion battery

ABSTRACT

A lithium polyacrylate (Li-PAA) binder has been developed by 3M Company that is useful with electrodes comprising alloy anode materials. This binder was used to prepare electrodes made with $\text{Sn}_{30}\text{Co}_{30}\text{C}_{40}$ material prepared by mechanical attrition. The electrochemical performance of electrodes using Li-PAA binder was characterized and compared to those using sodium carboxymethyl cellulose (CMC) and polyvinylidene fluoride (PVDF) binders. The $\text{Sn}_{30}\text{Co}_{30}\text{C}_{40}$ electrodes using Li-PAA and CMC binders show much smaller irreversible capacity than the ones using PVDF binder. Poor capacity retention is observed when PVDF binder is used. By contrast, the electrodes using Li-PAA binder show excellent capacity retention for $\text{Sn}_{30}\text{Co}_{30}\text{C}_{40}$ materials and a specific capacity of 450 mAh/g is achieved for at least 100 cycles. The results suggest that Li-PAA is a promising binder for electrodes made from large-volume change alloy materials.

© 2010 Elsevier Ltd. All rights reserved.

1. Introduction

Sn-based alloys have been intensively studied as negative electrode candidates for Li-ion batteries in the last decade because of their much higher specific and volumetric capacity compared with graphite [1–14]. However, they suffer from large-volume expansion during lithiation, which presents a huge challenge for capacity retention. Amorphous, nanoscale or nanostructured materials have been proposed to mitigate the capacity fading problem because they can eliminate the inhomogeneous expansion caused by the insertion of lithium atoms that occurs in crystalline materials [1]. Such candidates include nanostructured Si [2], amorphous $\text{Si}_{1-x}\text{Sn}_x$ [3], carbon-coated nanoparticles of Sn [4], Si/graphite nanocomposite [5], amorphous Si–Al–Fe [6], tin oxide nanocomposites [7], $\text{Sn}_2\text{Fe}/\text{SnFe}_3\text{C}$ nanocomposites [8], “amorphous” tin–cobalt–carbon (Sn–Co–C) [9–14] and so on. Among these materials, “amorphous” Sn–Co–C has been used in current commercial Li-ion cells [9] due to its excellent cycling performance and relative low-cost of mass production. It was suggested by Dahn et al. [10] that the addition of Co and C to Sn produces a nanostructured material that shows a stable structure on the atomic scale and thereby leads to a promising cycle life. Nanostructured Sn–Co–C can be prepared in bulk by

mechanochemical synthesis [11], which makes it commercially attractive.

From a practical point of view, Sn–Co–C alloy materials ultimately need to combine with carbon black and binder to make commercially viable negative electrodes. Although the optimization of alloy materials contributes significantly to overcome the problem of capacity fading due to particle cracking, capacity fading caused by huge volume changes is still present for composite electrodes with amorphous alloy materials because of the significant motions of particles within a composite electrode during cycling. For example, amorphous $\text{Si}_{64}\text{Sn}_{36}$ materials have good cycle life as binder-free sputtered films while amorphous $\text{Si}_{64}\text{Sn}_{36}$ composite electrodes using conventional PVDF binder show poor capacity retention [15]. It is believed that this problem is not caused by the active material itself, but by the polymeric binder that holds the active materials together. Therefore, the impact of binder selection on the performance of electrodes with alloy materials is significant.

Wagner et al. [16] first showed the importance of the binder choice on the cycling behavior of metallic alloys. Chen et al. [15,17] modified a poly(vinylidene fluoride-tetrafluoroethylene-propylene) elastomeric binder system to improve the capacity retention of amorphous $\text{Si}_{64}\text{Sn}_{36}$ composite electrodes. Liu et al. [18] then showed an enhanced cycle life of Si-based electrodes using sodium carboxymethyl cellulose (CMC)/styrene butadiene rubber (SBR) mixed binder compared to electrodes made using PVDF binder and attributed this success to the better mechanical properties of elastomeric SBR binder over PVDF binder. Li et al. [19] reported promising cycle life of Si electrodes made from crystalline

* Corresponding author at: Dept. of Physics, Dalhousie University, Halifax, N.S. B3H 3J5, Canada. Tel.: +1 902 494 2991; fax: +1 902 494 5191.

E-mail address: jeff.dahn@dal.ca (J.R. Dahn).

Si powder (–325 mesh) and CMC binder. Based on the fact that CMC is extremely stiff and brittle, it was suggested that mechanical properties are not the only factor that determines the performance of binders and other properties of binders such as surface modification need to be considered. Chen et al. [20] improved the cycling performance of 20% nanoscale Si-containing Si/C composite and nanoscale Si electrodes by replacing PVDF with acrylic adhesive binder. The performances were further enhanced by adding CMC because CMC was believed to help the distribution of the acrylic adhesive in the coating slurry, thereby improving the adhesion strength.

The interesting fact that brittle polymers like CMC can work well as binders for large-volume change alloy material attracted attention [5,21]. Guyomard and co-workers [21] studied the CMC and poly(ethylene-co-acrylic acid) blended-binder system for Si electrodes and claimed that the extended conformation of CMC in solution facilitates an efficient networking process between the conductive agent and Si particles. Winter and co-workers [5] reported that the chemical bonding between CMC binder and Si particles contributes to the enhanced capacity retention of Si/C composite electrodes.

Recently, electrochemically active polyimide-type binder was reported for Si-based electrodes [22,23]. It was suggested that an electrochemically active binder helps to maintain the electron conduction network during cycling [23]. Garsuch et al. [24] reported a promising cycling performance of Si electrodes by using a lithium-exchanged Nafion as a binder. Given that these binders are not elastomeric, it is believed that ionic conducting binders would be beneficial for the formation of a more effective solid electrolyte interphase (SEI) layer, which helps to improve the capacity retention of the alloy negative electrodes.

Not only the nature of the binder but also binder-related processing of the electrode such as electrode heat-treatment [24] and the solvent content of the electrode slurry [25] influence electrode cycling performance. These reports suggest that the composite electrode architecture, especially the distribution of the binder–carbon black network on the active material surface helps determine the electrochemical performance of the electrodes made from alloy materials.

The studies above clearly show that the choice of binder has a critical impact on the performance of composite electrodes with alloy materials. Recently, Dinh Ba Le at 3M Company developed a lithium polyacrylate (Li-PAA) binder which is useful in electrodes incorporating alloy anode materials [26]. Similar to CMC, polyacrylic acid (PAA) and its derivatives are often used as dispersants, thickeners and flocculants depending on their molecular weight [27]. They have been typically studied as a component of solid polymer electrolytes for alkaline batteries including Zn/MnO₂, Ni/MH, Ni/Cd, Ni/Zn and Zn/air batteries [28,29]. As for lithium-ion batteries, ammonium polyacrylate was proposed as a binder for LiCoO₂ positive electrodes to improve the slurry dispersion behavior and the rate capability [30]. In this work, Li-PAA was used to prepare negative electrodes made with Sn–Co–C material, prepared by mechanical attrition. Here the composition of Sn–Co–C material is Sn₃₀Co₃₀C₄₀, similar to that of the negative electrode used in new commercial lithium-ion cells (Nexelion, Sony [9]). A comparison of the Li-PAA binder with CMC and PVDF binders is presented and discussed.

2. Experimental

2.1. Active materials

The Sn₃₀Co₃₀C₄₀ samples were alloyed mechanically using a vertical-axis attritor (Union Process 01-HD attritor). Samples were

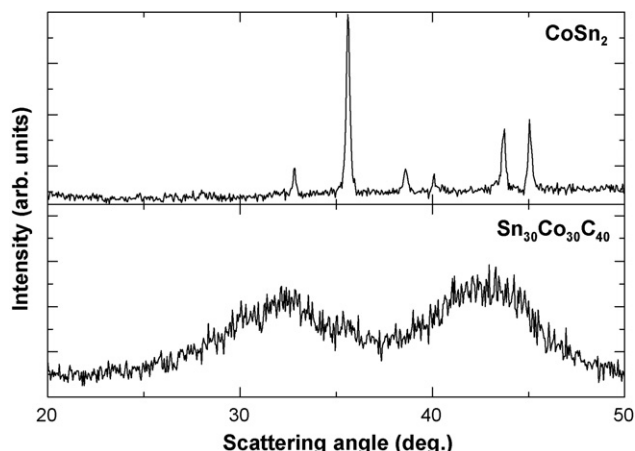


Fig. 1. XRD patterns of bulk CoSn₂ and attrited Sn₃₀Co₃₀C₄₀ powders. Bragg peaks of crystalline CoSn₂, as expected, are observed for the diffraction pattern of CoSn₂.

prepared from CoSn₂, Co (Sigma–Aldrich, <150 μm, 99.9+%) and graphite (Fluka, purum). The combination of these starting materials was selected due to the poor mechanical properties of elemental Sn powder in a high energy milling process [11]. If elemental Sn is used, chunks of materials are formed on the walls of the attritor can instead of a uniform powder. CoSn₂ was arc melted from elemental Sn (Sigma–Aldrich, <150 μm, 99.5%) and elemental Co followed by annealing at 500 °C for 24 h under flowing argon. The annealed material was then ground into powder and the X-ray diffraction (XRD) pattern of the resulting CoSn₂ powder, Fig. 1, showed no impurities. A powder charge of 25.0 g reactants (CoSn₂, Co and graphite) along with about 1400 0.25 in diameter stainless steels balls were loaded into the 700 mL stainless steel attritor can and sealed under an argon atmosphere. The mass ratio of powder to balls was 5:289. The angular velocity of the shaft was set at 700 RPM for a total duration of 16 h. More details about the starting material choices and the attritor system are available in Ref. [11].

The structure of attrited Sn₃₀Co₃₀C₄₀ powders was studied by XRD using a Siemens D-5000 diffractometer equipped with a Cu-target X-ray tube and a diffracted-beam monochromator. X-ray scans were collected from 10° to 90° in 0.05° increments at 5 s per point.

The particle size of the attrited Sn₃₀Co₃₀C₄₀ sample used was studied using a Hitachi S-4700 cold field-emission Scanning Electron Microscope (SEM). The Brunauer–Emmett–Teller (BET) surface area was determined with a Micromeritics Flowsorb II 2300 instrument using the single-point method.

2.2. Polymer binders

Three polymer binders were tested: (a) PVDF (9 wt% solution in N-methyl pyrrolidinone (NMP), NRC Canada), (b) CMC (CMC 2200, Daicel, Japan) and (c) Li-PAA binder synthesized in our laboratory. Li-PAA was made from poly (acrylic acid) (PAA) that was neutralized with lithium hydroxide. A stoichiometric amount of 10 wt% LiOH·H₂O (Sigma–Aldrich) solution was added to 25 wt% PAA solution (Alfa Aesar, average M.W. 240,000) according to a 1:1 mole ratio of LiOH to a monomeric unit of PAA. The mixture was stirred overnight. The formed solution was 11 wt% Li-PAA (100% Li salt–acid neutralized without excess) binder solution.

2.3. Preparation of electrodes

Measured amounts of active material, Super S carbon black (MMM Carbon, Belgium) and binder were added to an egg-shaped hardened steel vial according to the electrode formulation of 80 wt%

active material, 12 wt% carbon black and 8 wt% binder. Additional amounts of solvent (NMP for PVDF binder, water for CMC and Li-PAA binders) were added to give the mixture an appropriate viscosity. A shaker was used to shake the vials at 360 shakes/min for 30 min. Four 12 mm diameter hardened stainless steel balls served as mixing media. Then the slurries were spread on a copper foil with a 75 μm high notch bar. The wet electrodes were heated at 90 °C in air overnight to remove the water or organic solvent.

2.4. Electrochemical characterization

The $\text{Sn}_{30}\text{Co}_{30}\text{C}_{40}$ electrode served as the working electrode in a 2325-type coin cell using a lithium foil (FMC) disk as the counter and reference electrode. Two layers of microporous polypropylene separator (Celgard 2500) were used for each coin cell. For the $\text{Sn}_{30}\text{Co}_{30}\text{C}_{40}$ electrode, the electrolyte used was 1 M LiPF_6 in a mixed solution of EC and DEC (volume ratio = 1:2) with fluoroethylene carbonate (FEC, Fujian ChuangXin, China) added at 10% by weight to the electrolyte solvent. The coin cells were assembled and crimped closed in an Ar-filled glove box. The cells incorporating $\text{Sn}_{30}\text{Co}_{30}\text{C}_{40}$ electrodes were discharged from open circuit (near 2.7 V) to 0.005 V and then cycled between 1.2 and 0.005 V. The cells were cycled at a C/10 rate, as calculated prior from the expected theoretical capacity. The theoretical capacities of the Sn–Co–C attrited material was calculated assuming that only Sn and C are active with 4.4Li for every atom of Sn and 0.5Li for every C atom [10]. The electrochemical data were collected using a computer-controlled charger system manufactured by E-One Moli Energy Canada Ltd.

3. Results and discussion

Fig. 1 shows the XRD pattern of the $\text{Sn}_{30}\text{Co}_{30}\text{C}_{40}$ material as prepared by mechanical attrition. The diffraction pattern appears amorphous with two broad humps at about 32° and 43°, corresponding to an amorphous CoSn phase. This diffraction pattern is consistent with the model presented by Todd et al. [31] where amorphous CoSn grains are within a disordered carbon matrix. Fig. 2 shows SEM images of the attrited $\text{Sn}_{30}\text{Co}_{30}\text{C}_{40}$ used in our experiments. Fig. 2 shows that the average particle size of $\text{Sn}_{30}\text{Co}_{30}\text{C}_{40}$ is about 1 μm . The specific surface area is 0.6 m^2/g determined by BET methods. The use of low surface area materials is important for obtaining good thermal stability in commercial cells [32,33].

Fig. 3 shows potential vs specific capacity during the first five cycles for electrodes made with attrited $\text{Sn}_{30}\text{Co}_{30}\text{C}_{40}$ mate-

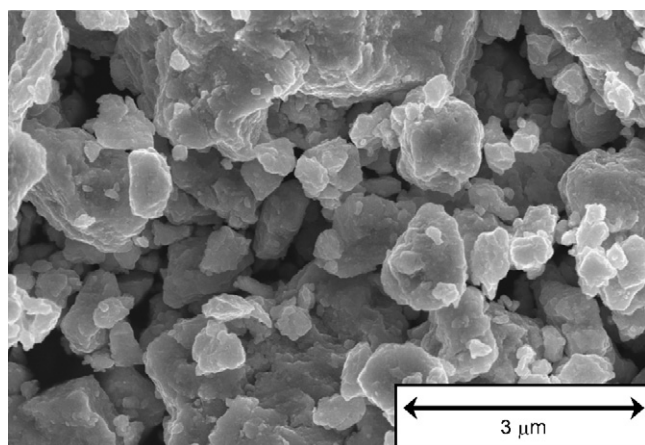


Fig. 2. SEM images of attrited $\text{Sn}_{30}\text{Co}_{30}\text{C}_{40}$ material.

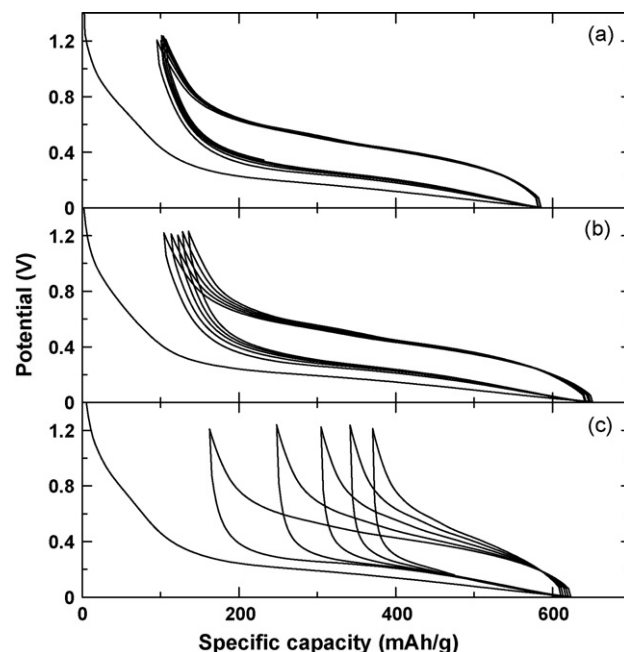


Fig. 3. Potential versus specific capacity for coin cells having $\text{Sn}_{30}\text{Co}_{30}\text{C}_{40}$ electrodes using different binders: (a) Li-PAA, (b) CMC and (c) PVDF as a binder. The electrolyte used here was 1 M LiPF_6 in a mixed solution of EC and DEC (volume ratio = 1:2) with FEC added at 10% by weight to the electrolyte solvent. Cells were charged and discharged between 0.005 and 1.2 V at C/10 rate.

rial using Li-PAA, CMC and PVDF binders. FEC was used here as the electrolyte additive at 10 wt% to the electrolyte solvent. The potential profiles for $\text{Sn}_{30}\text{Co}_{30}\text{C}_{40}$ electrodes using Li-PAA and CMC binders appear similar, showing an irreversible capacity of about 100 mAh/g. By contrast, the electrodes using PVDF binder show a higher irreversible capacity. For Li-PAA based electrodes, the shape of charge–discharge loops after the first discharge remains the same, indicating good capacity retention. The charge–discharge loops for CMC-based electrodes slowly shift to the right over five cycles, indicating a continuous capacity loss. The PVDF-based electrodes show the worst capacity retention, losing about 60% of the initial capacity after only 5 cycles.

Fig. 4 shows specific capacity vs cycle number for electrodes made with attrited $\text{Sn}_{30}\text{Co}_{30}\text{C}_{40}$ material using Li-PAA, CMC and PVDF binders. In terms of capacity retention, the $\text{Sn}_{30}\text{Co}_{30}\text{C}_{40}$

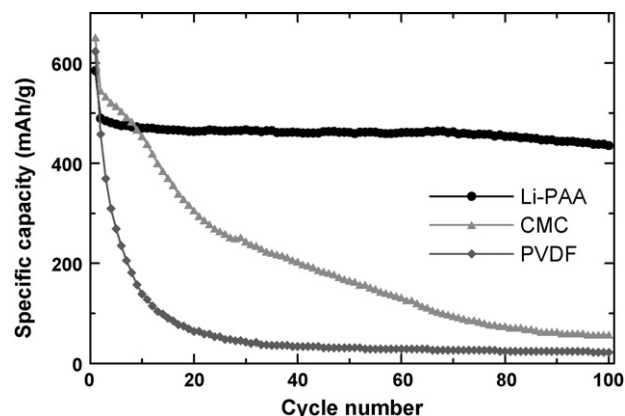


Fig. 4. Specific capacity versus cycle number for coin cells having $\text{Sn}_{30}\text{Co}_{30}\text{C}_{40}$ electrodes using Li-PAA, CMC and PVDF binders. The electrolyte used here was 1 M LiPF_6 in a mixed solution of EC and DEC (volume ratio = 1:2) with FEC added at 10 wt% to the electrolyte solvent. Cells were charged and discharged between 0.005 and 1.2 V at C/10 rate.

electrodes using different binders follow an increasing order of capacity retention: PVDF < CMC < Li-PAA. In particular, the electrodes using Li-PAA binder show excellent capacity retention after the first cycle, retaining a capacity of about 500 mAh/g for 90 cycles.

The $\text{Sn}_{30}\text{Co}_{30}\text{C}_{40}$ material used here is nanostructured as indicated in Fig. 1. Its potential profile shows no well-defined plateaus during lithiation/delithiation as shown in Fig. 3, characteristic of the amorphous nanometer-sized grains of CoSn within the carbon matrix. Although electrochemical pulverization is avoided due to the homogeneous expansion of the amorphous grains, the interparticle collisions and motions caused by enormous volume expansion up to 175% [14] upon full lithiation are still very challenging to the binder systems used to make such electrodes. Figs. 3 and 4 clearly show the importance of binder selection and suggest Li-PAA is a promising binder for electrodes made from Sn–Co–C material. Hassoun et al. [34] demonstrated an initial capacity of about 500 mAh/g and a capacity retention of about 60% for 100 cycles for electrodes made from $\text{Sn}_{31}\text{Co}_{28}\text{C}_{41}$ materials prepared by high energy ball milling and a PVDF binder. They ascribed the capacity decay to the degradation induced by binder. Based on the results shown in Figs. 3 and 4, an enhanced cycle life could be achieved for their materials if the PVDF binder is replaced by Li-PAA binder.

The huge difference between the performance of cells using an identical active material but with different binder systems stresses the point that the choice of binder is very important for composite electrodes made from active materials that have large-volume changes during cycling. PVDF works well for commercialized carbonaceous materials that have only 10% volume change. However, it shows very poor performance for large-volume expansion alloy materials such as the Sn–Co–C material shown here. Therefore, a proper binder needs to be chosen carefully when evaluating the performance of alloy negative electrode materials to avoid spurious conclusions.

As shown in Figs. 3 and 4, Li-PAA is a promising binder for alloy materials that have large-volume changes during cycling. Komaba et al. [35] showed polyacrylate (Li or Na salt) binder can suppress the co-intercalation of propylene carbonate into the graphite electrodes, suggesting that Li-PAA is an effective SEI layer modifier. It was also reported that the viscosity of PAA solution increases with neutralization [36], which indicates that Li-PAA can coat particle surface uniformly during the electrode preparation. Therefore, it is believed that Li-PAA can form a better ionic conductive film on the surface of active materials. During the first lithiation, this layer will help to form a more effective SEI layer, which thereby alleviates the continuous capacity loss and improves the cycling performance. Compared to PVDF that only becomes ion conducting after certain swelling with the electrolyte, the preliminary success of brittle binders such as CMC [19,5], Li-exchanged nafion [24] and Li-PAA reported here for electrodes made from alloy materials suggest that the enhanced capacity retention can be attributed to the binder-induced ion-conductive coating on the surface of alloy active materials that modifies the formation of SEI layer.

Besides, it was suggested that the improved cycle life of Si/C electrodes using CMC binder is mainly due to the chemical bonding between CMC and partially hydrolysed SiO_2 layer that covers Si particles [5]. Given that Li-PAA has carboxylic acid sites similar to that of CMC, Li-PAA may also has chemical interaction with alloy materials particles that usually have hydroxyl groups on the surface, thereby resulting in better capacity retention of the electrode incorporating Li-PAA binder.

Electrolyte additives such as FEC [37–39] have an important impact on the performance of electrodes made with alloy materials. This emphasizes again the significance of SEI modification for large-volume change alloy materials.

4. Conclusion

In summary, the electrochemical performance of $\text{Sn}_{30}\text{Co}_{30}\text{C}_{40}$ electrodes made using Li-PAA binder developed by 3M Company was compared to CMC or PVDF binders. This comparison clearly shows the impact of binder selection on the performance of negative electrodes made from alloy materials. $\text{Sn}_{30}\text{Co}_{30}\text{C}_{40}$ electrodes using different binders have an increasing order of capacity retention: PVDF < CMC < Li-PAA. In particular, the electrodes using Li-PAA binder retain over 450 mAh/g for 100 cycles.

These results show that Li-PAA is a promising binder for alloy negative electrodes. It was suggested that the use of Li-PAA binder leads to enhanced lithium-ion conductivity and electronic conductivity of the composite electrode, thereby improving the cycling performance. As a polyelectrolyte, Li-PAA may help to modify the formation of the SEI layer and thereby avoid continuous capacity loss on repeated cycling. Winter et al. [40] has published work on Si electrodes which use Li, Na or K–CMC binders. Each of these binders was shown to perform quite well. With that in mind we suggest that studies of Na-PAA and K-PAA binders should be made.

Acknowledgments

The authors acknowledge the support of this research by NSERC and 3M Canada under the auspices of the Industrial Research Chair program.

References

- [1] L.Y. Beaulieu, T.D. Hatchard, A. Bonakdarpour, M.D. Fleischauer, J.R. Dahn, *J. Electrochem. Soc.* 150 (2003) A1457.
- [2] J. Graetz, C.C. Ahn, R. Yazami, B. Fultz, *Electrochem. Solid-State Lett.* 6 (2003) A194.
- [3] T.D. Hatchard, M.N. Obrovac, J.R. Dahn, *J. Electrochem. Soc.* 153 (2006) A282.
- [4] J.Y. Lee, R. Zhang, Z. Liu, *J. Power Sources* 90 (2002) 70.
- [5] N.S. Hochgatterer, M.R. Schweiger, S. Koller, P.R. Raimann, T. Wöhrle, C. Wurm, M. Winter, *Electrochem. Solid-State Lett.* 11 (2008) A76.
- [6] M.D. Fleischauer, M.N. Obrovac, J.R. Dahn, *J. Electrochem. Soc.* 153 (2006) A1201.
- [7] Y. Idota, M. Mishima, Y. Miyaki, T. Kubota, T. Miyasaka, U.S. Pat. 5,618,640 (1997).
- [8] Ou Mao, J.R. Dahn, *J. Electrochem. Soc.* 146 (1999) 423.
- [9] <http://www.sony.net/SonyInfo/News/Press/200502/05-006E/>.
- [10] J.R. Dahn, R.E. Mar, A. Abouzeid, *J. Electrochem. Soc.* 153 (2006) A361.
- [11] P.P. Ferguson, A.D.W. Todd, J.R. Dahn, *Electrochem. Commun.* 10 (2008) 25.
- [12] A.D.W. Todd, R.E. Mar, J.R. Dahn, *J. Electrochem. Soc.* 154 (2007) A597.
- [13] A.D.W. Todd, P.P. Ferguson, M.D. Fleischauer, J.R. Dahn, *Int. J. Energy Res.*, in press, doi:10.1002/er.1669.
- [14] R.B. Lewis, A. Timmons, R.E. Mar, J.R. Dahn, *J. Electrochem. Soc.* 154 (2007) A213.
- [15] Z. Chen, L. Christensen, J.R. Dahn, *Electrochem. Commun.* 5 (2003) 919.
- [16] M.R. Wagner, M. Wachtler, M. Schmied, P. Preishuber-Pflugl, F. Stelzer, J.O. Besenhard, M. Winter, Abs #73 at 10th International Meeting of Lithium Batteries (IMLB 10), Como, Italy, 2000.
- [17] Z. Chen, L. Christensen, J.R. Dahn, *J. Electrochem. Soc.* 150 (2003) A1073.
- [18] W.R. Liu, M.H. Yang, H.C. Wu, S.M. Chiao, N.L. Wua, *Electrochem. Solid-State Lett.* 8 (2005) A100.
- [19] J. Li, R.B. Lewis, J.R. Dahn, *Electrochem. Solid-State Lett.* 10 (2006) A17.
- [20] L. Chen, X. Xie, J. Xie, K. Wang, J. Yang, *J. Appl. Electrochem.* 36 (2006) 1099.
- [21] B. Lestriez, S. Bahri, I. Sandu, L. Roué, D. Guyomard, *Electrochem. Commun.* 9 (2007) 2801.
- [22] M.N. Obrovac, L. Christensen, Dinh-Ba Le, Abs #19 at 14th International Meeting of Lithium Batteries (IMLB 14), Tianjin, China, 2008.
- [23] N.S. Choi, K.H. Yew, W.U. Choi, S.S. Kim, *J. Power Sources* 177 (2008) 590.
- [24] R.R. Garsuch, Dinh-Ba Le, A. Garsuch, J. Li, S. Wang, A. Farooq, J.R. Dahn, *J. Electrochem. Soc.* 155 (2008) A721.
- [25] E. Ligneel, B. Lestriez, A. Hudhomme, D. Guyomard, *J. Electrochem. Soc.* 154 (2007) A235.
- [26] Dinh Ba Le, U.S. Pat. Appl. 20080187838.
- [27] S. Chibowski, E. Grządka, J. Patkowski, *Colloids Surf.* 326 (2008) 191.
- [28] C. Iwakura, H. Murakami, S. Nohara, N. Furukawa, H. Inoue, *J. Power Sources* 152 (2005) 291.
- [29] X. Zhu, H. Yang, Y. Cao, X. Ai, *Electrochim. Acta* 49 (2004) 2533.
- [30] C. Li, J. Lee, C. Lo, M. Wu, *Electrochem. Solid-State Lett.* 8 (2005) A509.
- [31] A.D.W. Todd, R.A. Dunlap, J.R. Dahn, *J. Alloys Compd.* 443 (2007) 114.
- [32] Fu Zhou, Xuemei Zhao, P.P. Ferguson, J.S. Thorne, R.A. Dunlap, J.R. Dahn, *J. Electrochem. Soc.* 155 (2008) A921.
- [33] Y. Wang, J.R. Dahn, *Electrochem. Solid-State Lett.* 9 (2006) A340.

- [34] J. Hassoun, G. Mulas, S. Panero, B. Scrosati, *Electrochem. Commun.* 9 (2007) 2075.
- [35] S. Komaba, K. Okushi, T. Ozeki, A. Wakita, Y. Katayama, N. Tachikawa, T. Saito, H. Groult, Abs #625 at 14th International Meeting of Lithium Batteries (IMLB 14), Tianjin, China, 2008.
- [36] M. Masiak, W. Hyk, Z. Stojek, M. Ciszowska, *J. Phys. Chem. B* 111 (2007) 11194.
- [37] N.S. Choi, K.H. Yew, K.Y. Lee, M. Sung, H. Kim, S.S. Kim, *J. Power Sources* 161 (2006) 1254.
- [38] R. McMillan, H. Sleg, Z.X. Shu, W. Wang, *J. Power Sources* 81–82 (1999) 20.
- [39] J. Xu, W.H. Yao, Y.W. Yao, Z.C. Wang, Y. Yang, *Acta Phys.-Chim. Sin.* 25 (2009) 201.
- [40] M. Winter, A. Balducci, H. Damej, N.S. Hochgatterer, S. Koller, P.R. Raimann, M. Schmuck, M.R. Schweiger, M.O. Sternad, The 58th Annual Meeting of the International Society of Electrochemistry, Banff, Canada, September 9–14, 2007.